Protease-activated receptor-4 uses dual prolines and an anionic retention motif for thrombin recognition and cleavage

Suzanne L. JACQUES and Athan KULIOPULOS[1]

Molecular Cardiology Research Institute, Division of Hematology/Oncology, Tufts-New England Medical Center and Departments of Medicine and Biochemistry, Tufts University School of Medicine, Boston, MA 02111, U.S.A.

Thrombin activation of human platelets is mediated by the high-affinity PAR1 (protease-activated receptor-1) and the low-affinity PAR4 receptor. PAR1 and PAR4 exhibit markedly disparate kinetics of activation that likely reflect differences in the macromolecular association of thrombin with their respective N-terminal extracellular domains (exodomains). Here we examine the mechanism of initial thrombin binding and cleavage of the high- and low-affinity PAR exodomains using steady-state kinetic analyses. We showed that the PAR4 exodomain lacks the functional hirudin-like sequence found in PAR1 and does not bind exosite I to cause allosteric activation or inhibition of thrombin. Instead, PAR4 contains an anionic cluster, Asp^{57}...Asp^{59}...Glu^{62}...Asp^{65} (DDED), in its exodomain, which slows the dissociation of PAR4 from the cationic thrombin. The analogous anionic residues in the PAR1 exodomain do not influence affinity for thrombin. Although PAR4 is cleaved more slowly than PAR1 on the cell surface, peptides containing the PAR4 P_4-P_1 active-site-interacting sequence, Pro^{45}-Ala-Pro-Arg (PAPR), are efficiently cleaved due to the optimal placement of dual prolines at positions P_4 and P_2. In comparison, thrombin has low affinity and slow cleavage rates for peptides that have a P_3 proline as occurs in human PAR3. Thus, to compensate for the lack of exosite I binding, PAR4 utilizes proline residues in its P_4-P_1 sequence to provide high-affinity interactions with the active site and an anionic cluster to slow dissociation from the cationic thrombin.

Key words: G-protein coupled receptor (GPCR), kinetics, protease-activated receptor 1 (PAR1), protease-activated receptor 4 (PAR4), platelet, thrombin receptor.

INTRODUCTION

When a blood vessel is damaged, the coagulation protease thrombin quickly activates platelets and fibrinogen to form a haemostatic plug. Thrombin activates human platelets by cleaving the protease-activated receptors PAR1 and PAR4 at a specific peptide bond in the receptor exodomains. This cleavage creates a new N-terminus that binds to the body of the receptor in an unusual intramolecular liganding mode. In human platelets, PAR1 and PAR4 independently signal to intracellular G-proteins with distinct kinetics of activation and signal termination [1,2]. The Ca^{2+} signal from PAR1 is fast and shut off quickly, while activation of PAR4 gives a slow but pronounced Ca^{2+} transient. The initial velocity of Ca^{2+} flux is dependent on the affinity and rate of receptor cleavage by thrombin rather than efficiency of G-protein coupling, since at full occupancy with ligand (intra- or inter-molecular) PAR1 and PAR4 exhibit similar maximal initial rates of Ca^{2+} flux [1]. The slower PAR4 Ca^{2+} signal is dependent on the continuous presence of thrombin and is terminated upon addition of hirudin [1]. Therefore slow signalling by PAR4 is a direct consequence of its slow cleavage by thrombin. Despite its slower kinetics of activation, PAR4 contributes to the majority of the thrombin Ca^{2+} signal and, unlike PAR1, leads to irreversible platelet aggregation, even in the absence of an ADP-autocrine response [1].

The marked differences in the rates of activation of PAR1 and PAR4 likely reflect differences in the macromolecular association of thrombin with their respective N-terminal exodomains. For instance, previous studies showed that the PAR1 exodomain contains a Hir (hirudin-like sequence) element, K^{51}YEPF^{55}, that interacts with exosite I of thrombin [3]. Exosite I is a hydrophobic groove that is rimmed with cationic residues and is critical for strong interactions with physiological substrates and modulators of thrombin [4–7]. Exosite binding also plays an important role in substrate recognition for prothrombinase and extrinsic tenase [8,9]. Binding of the Hir of PAR1 or hirudin analogues at exosite I of thrombin causes marked allosteric effects (either enhancement or inhibition) on cleavage of small peptides that interact at the catalytic site [10,11]. Previously, we found that the initial binding of the Hir of PAR1 with exosite I is essential for rapid association to thrombin [11]. Following cleavage, thrombin remains tightly associated with the C-terminal portion of the PAR1 exodomain via this high-affinity Hir [11].

The PAR4 exodomain does not contain an obvious Hir and there is suggestive evidence that PAR4 may not bind exosite I of thrombin. PAR4 activation requires higher concentrations of thrombin than PAR1 [1,12,13] and γ-thrombin, a proteolytic product that lacks a functional exosite I, activates PAR4 as well as α-thrombin [12]. Furthermore, mutations in exosite I of thrombin (R67A, K70A, E80A) have much less impact on cleavage of a PAR4 exodomain peptide as compared with PAR1 [5]. A major question to be addressed is whether the disparate affinities of thrombin for PAR1 and PAR4 are due to the lack of productive binding of PAR4 to exosite I of thrombin, or are a consequence of differences in other thrombin-interacting sequences.

In this report, we directly measure thrombin cleavage of full-length PAR1 and PAR4 expressed on COS7 fibroblasts and the individual intrinsic kinetic properties of soluble PAR1 and PAR4 N-terminal exodomains. We found that PAR4 has optimized

Abbreviations used: Ac, acetyl; KSI, ketosteroid isomerase; PAR, protease-activated receptor; Hir, hirudin-like sequence; pNA, *p*-nitroanilide; CBS, CBS 34.47; PEG-8000, poly(ethylene glycol) 8000; MALDI, matrix-assisted laser-desorption ionization.

[1] To whom correspondence should be addressed (e-mail athan.kuliopulos@tufts.edu).

© 2003 Biochemical Society

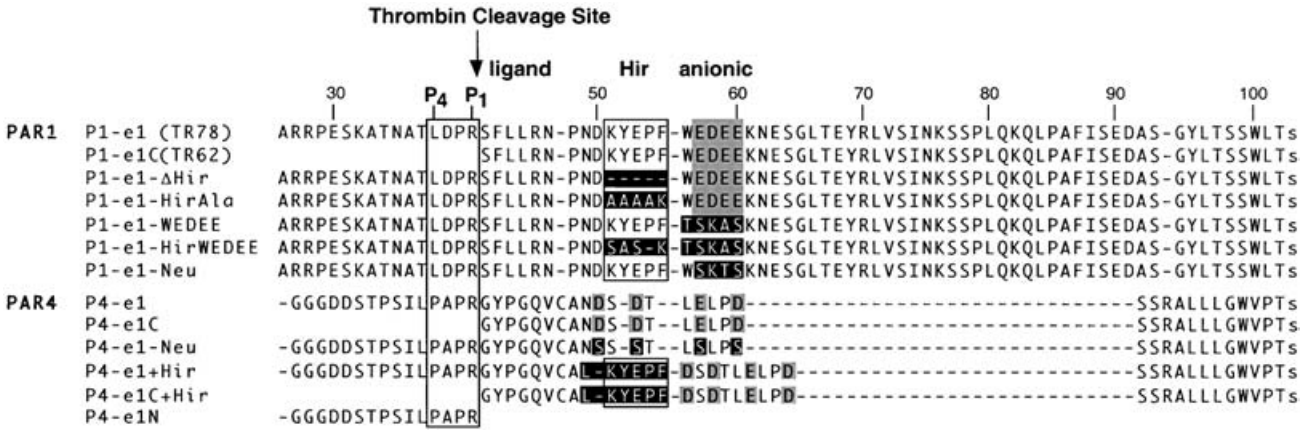

Figure 1 Amino acid sequences of the PAR1 and PAR4 N-terminal exodomains

Sequences are shown using the one-letter amino acid code; lower-case s indicates homoserine. Numbering is based on the PAR1 amino acid sequence numbering. Black boxes highlight the positions of mutations, grey boxes identify the clusters of negative residues and white boxes are drawn around the P_4-P_1 residues and the Hir sequence. The full-length (P1-e1) and C-terminal thrombin cleavage fragment (P1-e1C) of PAR1 were previously referred to as TR78 and TR62, respectively [11].

active-site binding by placement of an extra proline at the P_4 position. Unlike PAR1, the PAR4 exodomain does not induce allosteric effects on cleavage of peptides that bind the active site of thrombin, consistent with the notion that PAR4 lacks a functional Hir. However, we demonstrated that the negative residues found in the exodomain of PAR4 are used for prolonging interaction time with thrombin.

EXPERIMENTAL

Materials

Human α-thrombin was obtained from Hematologic Technologies (Essex Junction, VT, U.S.A.; specific activity, 2880 NIH units/mg). CBS (CBS 34.47; H-D-cyclohexylglycyl-L-α-aminobutyryl-L-arginine-*p*-nitroanilide) was purchased from American Bioproducts (Parsippany, NJ, U.S.A.) and H_2N-PAPR-pNA, *N*-Ac-PAPR-pNA, *N*-Ac-LPIK-pNA and *N*-Ac-LTIK-pNA (where Ac is acetyl and pNA is *p*-nitroanilide) were synthesized at the Kansas State University Biotechnology Core Laboratory (Manhattan, KS, U.S.A.). DMSO, potassium phosphate, PEG-8000 [poly(ethylene glycol) 8000], NaCl, sucrose and Tris/HCl were purchased from Sigma (St. Louis, MO, U.S.A.).

Thrombin cleavage of full-length PARs expressed on COS7 cells

The coding sequence for human PAR4 was amplified by PCR using primers containing 5′ *Kpn*I and 3′ *Xba*I restriction sites and pcDEF3-PAR4 [14] as a template. The coding sequence for the PAR1 signal sequence and the T7 tag was amplified from the PAR1AAA template [15] using primers containing 5′ *Bam*HI and 3′ *Kpn*I restriction sites. The amplified sequences were digested and ligated into the *Bam*HI/*Xba*I sites of the mammalian pcDEF3 expression vector to produce KE76, encoding T7-tagged PAR4. The resulting expression plasmid was sequenced to confirm the absence of erroneous mutations in the coding region. PAR1AAA, KE76 and pcDEF3 were transiently transfected into COS7 cells by DEAE-Dextran and grown for 48 h. The transfected COS7 cells were then washed with PBS, lifted with 1.5 mM EDTA/PBS, centrifuged at 200 ***g*** for 5 min and re-suspended in PBS to 1×10^5 cells/ml. Samples containing 5×10^4 transfected COS7 cells were incubated at 37 °C with various concentrations of human α-thrombin, the cleavage reactions were stopped with 0.15 units of hirudin and placed immediately on ice. Cells were then fixed with 1 % formaldehyde at 4 °C. The extent of receptor cleavage was determined by FACS using a T7 mouse monoclonal antibody (Novagen) and FITC-conjugated rabbit anti-mouse antibody (Zymed) by methods described previously [15].

Production of soluble PAR exodomains

The coding sequences for human PAR4 exodomain was amplified by PCR using primers containing 5′ *Nco*I and 3′ *Xho*I restriction sites and PAR4 cDNA EST (clone ID no. 2391725; IMAGE Consortium, Research Genetics) as a template. The reaction product was digested with *Nco*I and *Xho*I and ligated to the *Nco*I/*Xho*I sites of the pET31MØTR78 expression vector [11] to produce pETP4ED. Expression plasmids encoding the PAR exodomain mutants (pETP1-W, pETP1-KW, pETP1-E, pETP4+K, pETP4-S) were generated by the method in [16]. The sequences encoding the mutant exodomains were then subcloned into the *Nco*I/*Xho*I sites of the pET31MØTR78 expression vector. The expression plasmids were placed into *Escherichia coli* BL21 (DE3) *pLysS* for production of the PAR exodomain fusion proteins. The KSI (ketosteroid isomerase)-PAR-His_6 fusions were purified by Ni-chelate chromatography and the PAR exodomains were released from KSI and His_6 by CNBr cleavage and purified by reversed-phase HPLC as described in [15]. Molecular masses of the PAR exodomains were confirmed by MALDI (matrix-assisted laser-desorption ionization) MS.

Kinetics of thrombin cleavage of soluble PAR exodomains

Freeze-dried PAR exodomains, as illustrated in Figure 1, were reconstituted in 20 mM potassium phosphate buffer, pH 7.5, and 150 mM NaCl (PBS). PAR exodomain concentrations were determined by UV absorption of the exodomain tryptophan and tyrosine content at 278 nm [ε_{278} (P1-e1-Neu) = 15 200 $M^{-1} \cdot cm^{-1}$, ε_{278} (P1-e1-WEDEE) = 9700 $M^{-1} \cdot cm^{-1}$, ε_{278} (P1-e1-HirWEDEE) = 8300 $M^{-1} \cdot cm^{-1}$, ε_{278} (P4-e1) = 6900 $M^{-1} \cdot cm^{-1}$, ε_{278} (P4-e1-Neu) = 6900 $M^{-1} \cdot cm^{-1}$, ε_{278} (P4-e1+Hir) = 8300 $M^{-1} \cdot cm^{-1}$]. Thrombin cleavage of PAR exodomains was

© 2003 Biochemical Society

Table 1 Steady-state kinetic parameters for the cleavage of soluble PAR1 and PAR4 exodomains by thrombin

Conditions: 20 mM potassium phosphate, pH 7.5/150 mM NaCl, at 37 °C. The Gibb's free energy of activation ($\Delta G^{\ddagger}_{T}$) for the second-order rate constant, k_{cat}/K_m, was calculated from $\Delta G^{\ddagger}_{T} = RT[\ln(kT/h) - \ln(k_{cat}/K_m)]$ [35].

Substrate	K_m (μM)	k_{cat} (s^{-1})	k_{cat}/K_m ($M^{-1} \cdot s^{-1}$)	Fold decrease of k_{cat}/K_m	$\Delta G^{\ddagger}_{T}$ (kcal/mol)	$\Delta\Delta G^{\ddagger}_{T}$ (kcal/mol)
P1-e1*	26 ± 6	58 ± 6	2.2×10^6	1.0	9.2	0.0
P1-e1-ΔHir*	84 ± 17	22 ± 1	2.6×10^5	8.5	10.5	1.3
P1-e1-Neu†	21 ± 4	27 ± 2	1.3×10^6	1.7	9.5	0.3
P1-e1-WEDEE	56 ± 5	37 ± 0.9	6.6×10^5	3.3	9.9	0.7
P1-e1-HirWEDEE	121 ± 10	26 ± 0.7	2.1×10^5	10	10.6	1.4
P4-e1	56 ± 3	18 ± 0.3	3.2×10^5	6.9	10.4	1.2
P4-e1+Hir	55 ± 9	28 ± 1	5.1×10^5	4.3	10.1	0.9
P4-e1-Neu	208 ± 23	25 ± 1	1.2×10^5	18	11.0	1.8

* Data taken from [11].

† Values were normalized for the effects of DMSO using the equation $k_{corr} = k_{obs}/e^{-0.0243\ (\%\ DMSO)}$.

monitored by reversed-phase HPLC. Cleavage assays contained 5–510 μM exodomain in PBS and were conducted at 37 °C. Cleavages were initiated by the addition of human α-thrombin freshly diluted with ice-cold PBS/0.1 % PEG-8000 (final thrombin concentration, 0.36–2 nM). The final concentration of PEG-8000 in all of the assays was 0.009 %. The solubility of stock solutions of 220 μM P1-e1-Neu and 0.8-1 mM P1-e1-WEDEE was enhanced by the addition of 15 % or 1–3 % DMSO, respectively. Thrombin cleavage rates in the presence of > 1 % DMSO were corrected as indicated in Table 1.

Initial rates (k_{obs}) were obtained by analysing base-quenched samples taken at early time points where the progress curves were linear. Identification of cleavage products was determined by MALDI MS. Thrombin cleavage of PAR exodomains was monitored by measuring the generation of the N-terminal cleavage product [P1-e1N (A^{26}–R^{41}) or P4-e1N, Figure 1] at 222 nm. P1-e1N and P4-e1N were completely resolved from their respective undigested exodomains by reversed-phase HPLC. Quantification was performed by integrating peak areas and comparing them with calibration curves of fully digested samples. Initial rates were fitted to the Michaelis–Menten equation by non-linear least-squares regression to generate the kinetic parameters k_{cat} and K_m as before [11].

Kinetics of thrombin cleavage of chromogenic substrates

Chromogenic substrates (CBS, H_2N-PAPR-pNA, *N*-Ac-PAPR-pNA, *N*-Ac-LPIK-pNA and *N*-Ac-LTIK-pNA) were dissolved in 20 mM Tris/HCl, pH 8.3, and 150 mM NaCl (TBS). Solubility of stock solutions of 16 mM *N*-Ac-LPIK-pNA and 2.5 mM *N*-Ac-LTIK-pNA was enhanced by the addition of 3 % DMSO and 20 % methanol, respectively. Methanol concentrations below 20 % had no effect on thrombin activity. Cleavage assays comprised 10–1600 μM chromogenic substrate in TBS and were initiated by the addition of thrombin freshly diluted in ice-cold TBS/0.1 % PEG-8000 (final thrombin concentration, 0.21–80 nM) at 37 °C in a 96-well format. Initial rates were determined from the initial slopes of the progress curves using a SPECTRAmax 340 microplate spectrophotometer and SOFTmax PRO version 2.1. Quantification of pNA product was determined using the molar absorption coefficient $\varepsilon_{405} = 8300\ M^{-1} \cdot cm^{-1}$ and data were fitted to the Michaelis–Menten equation. Inhibition of thrombin cleavage of CBS by 5–150 μM PAR exodomains was performed at 24 °C. Inhibition data were tested against 12 inhibition models (linear, hyperbolic and parabolic models of competitive, non-competitive, uncompetitive and full non-competitive inhibition) by non-linear least-squares regression analysis as described in detail in [11].

Effect of solution viscosity on PAR exodomain cleavage by thrombin

Assays were performed as above in the presence of 0–25 % sucrose viscogen. Relative viscosity (η_{rel}) of the assay solution was measured relative to PBS alone in quadruplicate using an Ostwald viscometer. Initial velocities were fitted to the Michaelis–Menten equation and the kinetic parameters were analysed as a function of relative viscosity. Because solution viscosity affects the rates of diffusion-controlled steps, such as substrate association and dissociation, one can define the parameters shown in the following one substrate reaction:

$$E + S \underset{k_d}{\overset{k_a}{\rightleftharpoons}} ES \xrightarrow{k_f} E + P \quad (1)$$

where k_a is the rate constant of substrate association, k_d is the rate of substrate dissociation, k_f is the rate of conversion to product and includes dissociation of product from enzyme, E is the enzyme, S is the substrate, ES is the enzyme–substrate complex and P is the product. Ideally, rates of steps not controlled by diffusion, such as a conformational change or a chemical reaction step, will remain unaffected by relative solution viscosity [17,18]. Association rate constants (k_a) and 'stickiness' ratios ($S_r = k_f/k_d$) were determined for the PAR exodomains by fitting the viscosity data to eqn (2) using linear regression analysis as before [11]:

$$1/(k_{cat}/K_m) = \eta_{rel}/k_a + (k_d/k_f)/k_a \quad (2)$$

RESULTS

Relative cleavage efficiencies of thrombin for full-length PAR1 and PAR4 expressed on COS7 fibroblasts

Previous studies measuring intracellular Ca^{2+} flux indicate that PAR4 is activated more slowly than PAR1 [1]; however, the relative rates of proteolytic cleavage have not been directly measured. In order to determine the relative cleavage efficiencies of thrombin for full-length human PAR1 and PAR4, we placed a T7 epitope on the N-terminus of the receptors and expressed the receptors at equal levels in COS7 fibroblasts. As shown in Figure 2, PAR4 is cleaved by thrombin with ⩾100-fold lower apparent affinity than PAR1. The EC_{50} value for thrombin cleavage of PAR1 is close to the estimated PAR1 concentration in transfected fibroblasts (0.5–1.0 nM [19]); therefore, it is possible that thrombin is titrating PAR1 on the surface of fibroblasts. If this is the case, then one would predict that an increase in PAR1 expression would require more thrombin to achieve stoichiometry which would result in a higher (right-shifted) EC_{50} of cleavage. In fact, increasing PAR1 (or PAR4 expression) by 2-fold resulted in increased cleavage by thrombin (Figure 2), reflecting a lower EC_{50}. These data are consistent with the assertion that the EC_{50} primarily reflects the efficiency of cleavage of PAR1 and PAR4 by thrombin rather than stoichiometric titration. In order to directly measure the intrinsic kinetic properties of PAR4 by varying the substrate concentration rather than the enzyme concentration, we conducted kinetic studies using full-length soluble PAR4 exodomains.

© 2003 Biochemical Society

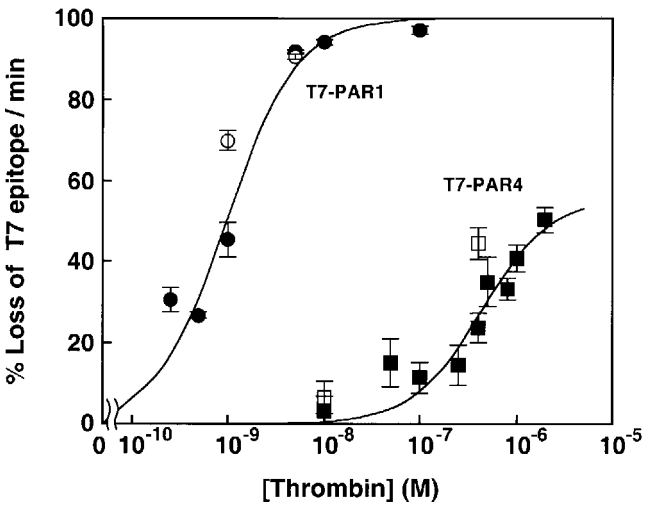

Figure 2 Relative cleavage efficiencies of thrombin for full-length PAR1 and PAR4 expressed on the surface of COS7 fibroblasts

T7-tagged PAR1 (●) and T7-tagged PAR4 (■) were transiently expressed at equal levels in COS7 cells and treated with thrombin at 37 °C in PBS. Receptor cleavage was monitored as loss of T7 epitope by FACS. The percentage of PAR cleaved by thrombin over 1 min is plotted against thrombin concentration. Surface expression levels were determined from the mean fluorescence intensity during FACS analysis and compared with vector-transfected control cells. Surface cleavage reactions were also conducted on cells expressing 2-fold higher levels of PAR1 (○) or PAR4 (□). Data are means ± S.E.M. from two or three separate experiments. The solid lines represent the best fit to a one-site dose-response curve. EC_{50} values for PAR1 and PAR4 are 1.0 ± 0.2 and 440 ± 150 nM, respectively.

Comparison of the thrombin specificities and association rates of the PAR1 and PAR4 exodomains

PAR1 and PAR4 have relatively low sequence identity (13–18 %) in their N-terminal exodomains (Figure 1), yet these domains contain all of the necessary sites for interaction with thrombin [19,20]. To understand the molecular basis of how PAR4 is recognized and cleaved by thrombin in comparison with PAR1 [11], we conducted steady-state kinetic measurements of association/dissociation and cleavage of the soluble PAR4 exodomain, P4-e1 (Figure 1), by thrombin. We found that P4-e1 has a second-order rate constant (k_{cat}/K_m) of 3.2×10^5 $M^{-1} \cdot s^{-1}$, which is nearly identical to a previously determined value of 3.4×10^5 $M^{-1} \cdot s^{-1}$ for a shorter PAR4 exodomain peptide [5]. The PAR4 exodomain has a 7-fold lower specificity for thrombin relative to the PAR1 exodomain, P1-e1 (Table 1), as a result of a 2-fold higher K_m and a 3-fold lower k_{cat}.

The initial binding events of thrombin to the exodomain preceding cleavage were then examined by measuring the effect of solution viscosity on the reaction kinetics. The stickiness ratio, which is the ratio of the rate of forward conversion to product over the rate of dissociation (k_f/k_d), approaches zero for 'non-sticky' substrates, which undergo rapid equilibrium binding, and approaches infinity for 'sticky' substrates [17]. The low stickiness ratio (S_r) of 0.22 (Table 2) for the P4-e1 exodomain demonstrates that, like PAR1 [11], PAR4 achieves rapid equilibrium binding with thrombin. Therefore, the forward rate of conversion to product, k_f, is much slower than the dissociation rate back to free exodomain and thrombin. Thrombin binding to these PARs is in marked contrast with thrombin binding to fibrinogen, which behaves as a sticky substrate [18]. These viscosity experiments also determined that the PAR4 exodomain associates (k_a) 12-fold more slowly to thrombin relative to PAR1 (Table 2). Thus thrombin cleaves the PAR4 exodomain less efficiently than PAR1 as a result of lower rates of forward association and cleavage.

Table 2 Association rate constants (k_a) and stickiness ratios (S_r) determined from the effect of relative solution viscosity (η_{rel}) on the cleavage of soluble PAR exodomains by thrombin

Conditions: 20 mM potassium phosphate, pH 7.5/150 mM NaCl, at 37 °C. The concentrations of sucrose viscogen used here (0–25 %) were previously shown to produce no macroscopic effects on thrombin activity (e.g. dielectric coefficient, volume exclusion, interactions with sucrose) as assessed by the cleavage of the PAR1 exodomain (TR78) or small chromogenic substrates [11]. S_r is the stickiness ratio of k_f/k_d. The Gibb's free energy of activation ($\Delta G^{\ddagger}_T$) for the second-order association constant, k_a, was calculated from $\Delta G^{\ddagger}_T = RT[\ln(kT/h) - \ln(k_a)]$ [35].

Substrate	S_r	k_a ($M^{-1} \cdot s^{-1}$)	Fold decrease of k_a	$\Delta G^{\ddagger}_T$ (kcal/mol)	$\Delta\Delta G^{\ddagger}_T$ (kcal/mol)
P1-e1*	0.12	1.9×10^7	1.0	7.8	0.0
P1-e1-ΔHir*	73	2.6×10^5	73	10.5	2.7
P1-e1-WEDEE†	1.4	1.3×10^6	15	9.5	1.7
P4-e1	0.22	1.6×10^6	12	9.4	1.6
P4-e1-Neu	0.06	2.2×10^6	8.6	9.2	1.4

* Data taken from [11].
† S_r and k_a are estimated for P1-e1-WEDEE, since there is a viscosity effect on k_{cat} [17].

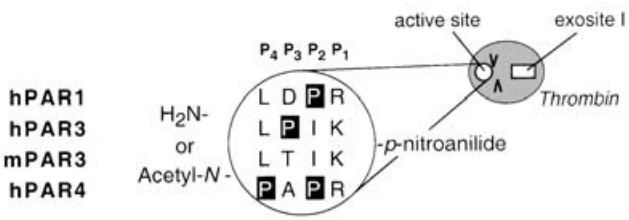

Figure 3 Amino acid sequences of the chromogenic P_4-P_1 PAR peptides

Placement of the P_4-P_2 prolines determines the specificity of the PARs to the active site of thrombin

We noted that each of the thrombin receptors has a distinct placement of proline residues in the P_4-P_2 positions that interact with the active site of thrombin (Figure 3). In order to determine whether the active site-interacting residues are responsible for lower substrate specificity of PAR4 for thrombin, steady-state kinetics of chromogenic peptides containing the P_4-P_1 residues of PAR4 were compared with the corresponding PAR1-derived peptide [11]. Both PAR1 and PAR4 contain a proline residue at the P_2 position, which has been shown to be the most efficient residue at position P_2 for thrombin specificity in the context of short peptide substrates [21,22]. PAR1 contains a leucine at P_4, whereas PAR4 contains an additional proline at this position. Although leucine has been proposed to be the optimal residue at position P_4 [22,23], we found that the PAR4 peptide, **P**APR, had 2-fold higher affinity (Table 3) relative to the analogous PAR1 peptide, **L**DPR.

We tested the effect of removal of the N-terminal acetyl group from the PAR4 chromogenic peptide, since binding of PAR4 to thrombin was previously shown to be dependent on hydrophobic interactions with leucine in position P_5 of the PAR4 exodomain [5]. Favourable hydrophobic interactions may therefore occur with the N-terminal acetyl group acting as a surrogate P_5 residue. By contrast, thrombin forms hydrophobic interactions with the

© 2003 Biochemical Society

Table 3 Steady-state kinetic parameters for the cleavage of chromogenic P_4-P_1 PAR peptides by thrombin

Conditions: 20 mM Tris/HCl, pH 8.3/150 mM NaCl, at 37 °C.

Receptor	Substrate	K_m (μM)	k_{cat} (s^{-1})	k_{cat}/K_m ($M^{-1} \cdot s^{-1}$)	Fold decrease of k_{cat}/K_m
hPAR1*	*N*-Ac-LDPR-pNA	113 ± 11	119 ± 5	1.1×10^6	1.0
hPAR3	*N*-Ac-LPIK-pNA	1800 ± 100	1.0 ± 0.04	5.6×10^2	2000
mPAR3	*N*-Ac-LTIK-pNA	250 ± 25	2.2 ± 0.1	8.7×10^3	125
hPAR4	*N*-Ac-PAPR-pNA	61 ± 4	81 ± 1	1.3×10^6	0.85
hPAR4	H_2N-PAPR-pNA	270 ± 49	49 ± 4	1.8×10^5	6.1

* Data taken from [11].

P_4 leucine in PAR1 [5]. Removal of the N-terminal acetyl group gave a 7-fold loss on k_{cat}/K_m for the PAR4 peptide (Table 3) versus a 1.6-fold increase for the PAR1 peptide [11]. This suggests that the presence of a P_4 proline in PAR4 significantly alters the geometry and binding of the adjacent active-site-interacting residues to thrombin [24].

Interestingly, PAR3 is the only one of the three human thrombin receptors to lack a P_2 proline and instead has a single P_3 proline. Indeed, we found that the PAR3 peptide, *N*-Ac-LPIK-pNA, is a very poor substrate for thrombin. It is cleaved 120-fold more slowly and has a 16-fold poorer affinity as compared with the PAR1 chromogenic substrate (Table 3). Strikingly, relative specificity (k_{cat}/K_m) is 2000-fold greater for the PAR1 versus the PAR3 chromogenic substrates. The mouse PAR3 P_4-P_1 peptide completely lacks prolines and was also tested. The mouse PAR3 peptide, *N*-Ac-LTIK-pNA, is cleaved 2-fold faster ($k_{cat} = 2.2\ s^{-1}$) and binds 7-fold more tightly ($K_m = 250\ \mu$M) relative to its human counterpart, but is still 125-fold less specific for thrombin relative to the PAR1 peptide.

PAR4 does not contain a Hir that allosterically modulates thrombin

Previously, we showed that the PAR1 exodomain, P1-e1, exhibited non-competitive inhibition of thrombin as a result of binding to two distinct sites, the active site and exosite I [11]. PAR1 binding to exosite I of thrombin was detected as allosteric inhibition of chromogenic peptide cleavage at the active site. Other studies have also shown that binding of thrombin modulators to exosite I or exosite II cause either positive or negative allosteric effects on cleavage of small peptide substrates [10,25–27]. Deletion or substitution of the Hir (P1-e1-ΔHir, P1-e1-HirAla) in PAR1 resulted in the loss of allosteric interactions with exosite I of thrombin, as indicated by the corresponding loss of noncompetitive inhibition [11]. To determine whether the PAR4 exodomain induces allosteric effects on thrombin, we conducted inhibition studies against a small thrombin-optimized chromogenic substrate, CBS. The data were tested against 12 inhibition models (linear, hyperbolic and parabolic models of competitive, non-competitive, uncompetitive and full non-competitive inhibition) by non-linear least-squares regression analysis and the best fits were chosen (Table 4). P4-e1 clearly displayed linear competitive inhibition with a K_{is} value of $26\ \mu$M, suggesting that this exodomain only binds the active site of thrombin. The N- and C-terminal thrombin cleavage products of the PAR4 exodomain (Figure 1) were then tested for the ability to inhibit thrombin. The C-terminal thrombin-cleavage fragment of PAR4, P4-e1C, did not affect proteolysis of CBS (Table 4), *N*-Ac-LDPR-pNA or *N*-Ac-PAPR-pNA (results not shown), suggesting that PAR4 does not induce allosteric effects via a Hir-like interaction with

Table 4 Inhibition of thrombin cleavage of CBS by soluble PAR1 and PAR4 exodomains

Conditions: 20 mM Tris/HCl, pH 8.3/150 mM NaCl, at 24 °C. NC, full non-competitive inhibition, where $K_{ii} = \alpha K_{is}$; UC, uncompetitive inhibition; NI, no inhibition (up to 100 μM exodomain concentrations); C, competitive inhibition.

Exodomain	Inhibition type	K_{is} (μM)	K_{ii} (μM)
P1-e1*	NC	2.4 ± 0.4	21 ± 8
P1-e1C*	UC	9 ± 2	
P1-e1-ΔHir*	NI		
P1-e1-HirAla*	C	35 ± 6	
P1-e1-WEDEE	NC	27 ± 7	238 ± 85
P1-e1-HirWEDEE	C	37 ± 6	
P4-e1	C	26 ± 4	
P4-e1C	NI		
P4-e1+Hir	C	33 ± 8	
P4-e1C+Hir	NI		
P4-e1-Neu	C	113 ± 20	
P4-e1N	NI		

* Data taken from [11].

exosite I of thrombin, as occurs with PAR1 (Table 4). Likewise, the N-terminal thrombin-cleavage fragment, P4-e1N, was not an inhibitor of thrombin activity, as seen previously with the N-terminal fragment of PAR1 [11]. Competitive inhibition by P4-e1 and the lack of inhibition by P4-e1C suggests that the PAR4 exodomain binds predominantly to the active site of thrombin under steady-state conditions.

We then tested whether insertion of the minimal Hir (KYEPF) from PAR1 into PAR4 (P4-e1+Hir; Figure 1) would confer exosite I binding to thrombin (Tables 1 and 4). Cleavage of P4-e1+Hir by thrombin gave similar kinetic parameters ($k_{cat} = 28\ s^{-1}$, $K_m = 55\ \mu$M) as wild-type PAR4 exodomain. The P4-e1+Hir mutant retained a competitive pattern of thrombin inhibition with K_{is} of $33\ \mu$M, while its C-terminal thrombin-cleavage fragment, P4-e1-C+Hir, did not inhibit thrombin, akin to the wild-type P4-e1 and P4-e1-C exodomains respectively. Therefore insertion of the Hir KYEPF motif from PAR1 into the PAR4 exodomain did not confer allosteric behaviour or increase cleavage rate or affinity for thrombin. This is in contrast to a previous report [20] where insertion of a large fragment (26 amino acids) containing the mouse PAR3 Hir and flanking residues into mouse PAR4 enhanced receptor cleavage. It is possible that the chimaeric P4-e1+Hir domain lacks the proper spacing between the P_4-P_1 residues and the Hir or that other structural determinants in the much shorter PAR4 exodomain prevent interactions of the inserted Hir with exosite I.

An anionic cluster in PAR4 slows the rate of dissociation away from thrombin

Although we have shown that PAR4 does not contain a Hir that can induce allosteric effects, PAR4 does include a cluster of negatively charged residues (Asp^{57}...Asp^{59}...Glu^{62}...Asp^{65}) located in the middle of the exodomain that might interact with the cationic residues at or near exosite I of thrombin [5,28]. In order to determine the potential function of these anionic residues in PAR4, the negative charges were substituted with uncharged or positive residues and the cleavage kinetics of the neutralized (Neu) exodomain (Figure 1) were determined. Neutralization of the DDED motif in the PAR4 exodomain, P4-e1-Neu, gave a 4-fold loss in affinity and a slight increase in k_{cat} (Table 1). P4-e1-Neu also lost 4-fold affinity as a competitive

© 2003 Biochemical Society

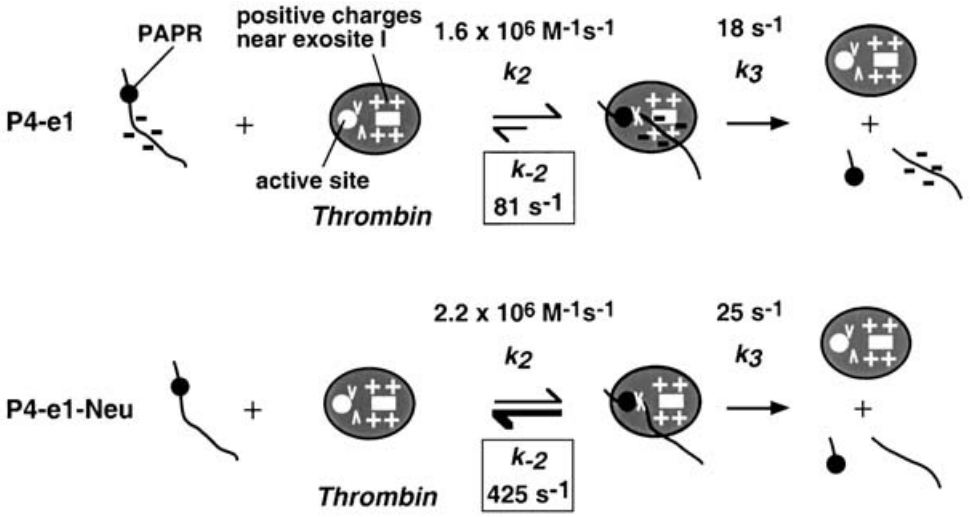

Figure 4 PAR4 uses an anionic retention mechanism to slow dissociation from thrombin

inhibitor of thrombin cleavage of the CBS chromogenic substrate (Table 4). Importantly, neutralization of the anionic cluster did not slow the forward rate constant of association, k_a, of the PAR4 exodomain with thrombin (Table 2). Hence, these negative residues in the PAR4 exodomain control its affinity to thrombin by selectively slowing the rate of dissociation, k_d, and thereby prolonging the interaction time (Figure 4).

Tryptophan residue 56 in the PAR1 exodomain is more important than the adjacent cluster of anionic residues for increasing affinity of the Hir for thrombin

Like PAR4, PAR1 contains a region of negative residues located just to the C-terminal side of the Hir. Similarly, the negative residues, $E^{57}DEE^{60}$, in PAR1 were substituted with uncharged or positive residues and the cleavage kinetics of the neutralized (P1-e1-Neu) PAR1 exodomain (Figure 1) determined. In contrast to PAR4, mutation of the negative residues in the PAR1 exodomain did not affect the affinity for thrombin (Table 1).

However, PAR1 contains a tryptophan residue at position 56 that serves as a hydrophobic scaffold for the flanking $K^{51}YEPF^{55}$ region, as determined by NMR structural analysis [29]. Mutation of the entire $W^{56}EDEE^{60}$ sequence (P1-e1-WEDEE) reduced the specificity (k_{cat}/K_m) of the PAR1 exodomain for thrombin by 3-fold with a 2-fold increase in K_m (Table 1). This result is consistent with previous studies where a W56A mutation in the full-length PAR1 receptor gave 70% activity of wild-type receptor [30]. Substitution of both the Hir and WEDEE sequence produced a defective PAR1 exodomain (P1-e1-HirWEDEE) with kinetic parameters very similar to the Hir deletion mutant, P1-e1-ΔHir (Table 1). Therefore neutralizing only the negative residues on PAR1 had very little effect on thrombin affinity as compared with mutating the Hir or the scaffolding residue W^{56} in conjunction with $E^{57}DEE^{60}$.

Lastly, we showed that the P1-e1-WEDEE mutant exhibited the same non-competitive inhibition pattern seen with the wild-type P1-e1 exodomain (Table 4), although with 11-fold weaker K_i values ($K_{is} = 27\ \mu M$, $K_{ii} = 238\ \mu M$). Inhibition of thrombin-catalysed CBS cleavage by P1-e1-HirWEDEE was competitive with a K_{is} of 37 μM, similar to P1-e1-HirAla. These results indicate that the interaction of PAR1 with exosite I of thrombin is dependent upon the presence of the Hir, and that the adjacent hydrophobic scaffolding residue W^{56} increases the affinity of the Hir for exosite I by up to 11-fold.

DISCUSSION

Here, we show that PAR4 uses a unique molecular strategy to interact with thrombin that differs considerably from PAR1. The much shorter PAR4 exodomain is bereft of a Hir, which is present in PAR1 [29,30] and, as such, does not induce allosteric effects on thrombin. Moreover, the forward rate of association, k_a, of thrombin to PAR4 is 12-fold slower relative to PAR1. Cleavage of PAR4 was also reduced by 7-fold relative to the PAR1 exodomain and could not be enhanced by the insertion of the PAR1 Hir. Together, these data indicate that the lower specifity of thrombin for PAR4 is due to the lack of productive binding to exosite I of thrombin.

Although PAR4 does not contain a functional Hir motif, a cluster of negative residues, DDED, in the PAR4 exodomain was found to enhance the affinity for thrombin by 4-fold. Mutation of these negative residues had no effect on the forward rate constant of association (k_a). Instead, the affinity of PAR4 for thrombin was enhanced by slowing the rate of dissociation (k_d) thereby increasing the interaction time. This anionic cluster in PAR4 may form electrostatic interactions with the positive residues (Arg^{67}, Lys^{70}, Arg^{73}) that rim exosite I [5] without causing allosteric effects at the catalytic site. The analogous negative residues ($E^{57}DEE^{60}$) in PAR1 do not appear to have the same function, since no change in affinity was detected upon neutralization of these residues. Likewise, mutation or deletion of the anionic cluster in full-length PAR1 had no effect on receptor activation [30]. Therefore PAR1 relies predominantly on the hydrophobic Hir [29,30], whereas PAR4 utilizes the anionic DDED motif for macromolecular interactions.

Surprisingly, a chromogenic peptide comprising the active site-binding sequence of PAR4, $P^{45}APR$, is the highest-affinity small-peptide substrate of the three thrombin receptors and is the most efficiently cleaved by thrombin due to the optimal placement of prolines in the P_4 and P_2 positions. In comparison, thrombin exhibited the lowest affinity for the human PAR3 L^{35}**PIK** sequence, which we attributed to the awkward placement of a proline at position P_3. The mouse PAR3 P_4-P_1 sequence, $L^{34}TIK$,

© 2003 Biochemical Society

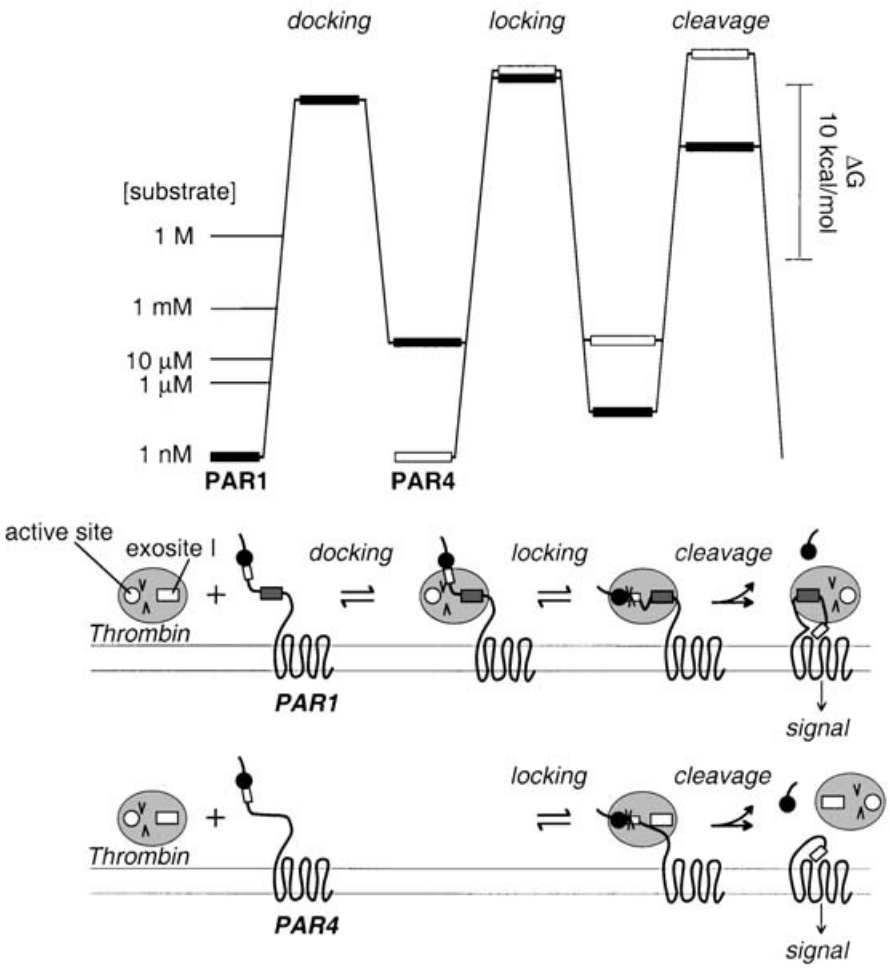

Figure 5 Energetics of thrombin interactions and cleavage of PAR1 and PAR4

A two-step dock-and-lock mechanism is shown for thrombin cleavage of PAR1 [11]. The individual steps of the dock-and-lock mechanism are illustrated as an energy diagram (top) and are aligned with the mechanisms below. The energy diagram was constructed using Gibb's free energies of activation ($\Delta G^{\ddagger}_{T}$) calculated from the equation $\Delta G^{\ddagger}_{T} = RT[\ln(kT/h) - \ln(k)]$ [35], using the kinetic parameters k_{cat}/K_m and k_{cat} and the individual rates shown in Figure 4 for P4-e1. The rate constants for PAR1 were previously determined [11]. The rate constants of PAR4 in Figure 4 were determined as follows: association rate constant (k_a) for P4-e1 was directly determined in viscosity studies and correspond to k_2 respectively. The maximal cleavage rate (k_{cat}) of P4-e1 by thrombin is determined by k_3. As an initial estimate, we assumed that the stickiness ratio ($S_r = 0.22$) is equal to k_2/k_{-1} ($k_{-1} = 82\ s^{-1}$). The remaining value, k_{-2}, for P4-e1 was determined by fitting the initial rate data to the Michaelis–Menten equation using Kaleidograph where: $K_m = (k_3 + k_{-2})/k_2$ for P4-e1 [16], allowing the other parameters to float from their initial values. The black boxes represent the energetics for PAR1, the white boxes represent the energetics for PAR4. The concentration scale on the left depicts the energies of the initial substrate concentrations.

lacks the P_3 proline and as a consequence has a 16-fold higher cleavage rate for thrombin, however, the specificity remains poor due to the missing preferred proline at position P_2. Human and mouse PAR3 also contain a P_1 lysine residue instead of arginine. Substitution of the P_1 arginine for lysine was previously shown to have much less effect on thrombin specificity than substitution of the proline residue at P_2, and the effect of the P_1 lysine is dependent on the residue at position P_2 [21,31]. For example, the specificity of thrombin for small peptides containing a P_1 lysine was 25- and 67-fold lower than for peptides with a P_1 arginine, when the peptides contained proline or leucine at position P_2, respectively [21]. In contrast, replacement of proline at position P_2 with leucine or glycine caused a 800–900-fold reduction in thrombin-cleavage rates [21]. Therefore, the lysine at P_1 may contribute to a portion of the 125-fold decreased specificity of mouse PAR3 (LTIK) for thrombin but does not account for the 2000-fold slower cleavage of human PAR3 (LPIK). Hence, placement of proline at position P_3 in human PAR3, or the lack of proline at P_2 in human and mouse PAR3, appears to be detrimental to thrombin activity. Together, these results show that the placement of proline residues in the P_4-P_2 sites of PAR1, PAR3 and PAR4 is critical for specificity to the active site of thrombin.

The steady-state kinetic and viscosity data for the PAR1 exodomain was previously fitted to a two-step dock-and-lock mechanism (Figure 5) that describes the steps leading to cleavage [11]. In this mechanism, the high-affinity Hir first docks to exosite I of thrombin followed by intramolecular locking of the P_4-P_1 sequence to the active site [11]. Peptide cleavage at the Arg^{41}-Ser^{42} scissile bond is allosterically enhanced by the Hir docked to exosite I. Because PAR4 lacks a Hir, a simple one-step binding reaction was used here (Figure 5). The reaction rates for the wild-type PAR4 exodomain in this scheme were converted to Gibb's free energies of activation ($\Delta G^{\ddagger}_{T}$) and are represented as an energy diagram. These energetics of PAR4 binding and cleavage are overlaid on to the previously determined two-step PAR1 reaction scheme. We postulate that PAR4 first interacts with thrombin using its optimized PAPR P_4-P_1 sequence. This association/locking step requires a greater energy of activation relative to the docking of thrombin to the high-affinity Hir of PAR1. The shortened PAR4 exodomain (Figure 1) may assist in

© 2003 Biochemical Society

this process by reducing entropic degrees of freedom. The ground state of the active site-bound PAR4 is at a considerably higher energy level than the locked PAR1 exodomain, demonstrating the amount of energy stabilization that is derived from exosite I interactions with the PAR1 Hir. The anionic sequence of PAR4 stabilizes the locked ground state and slows the rate of dissociation back to free exodomain and thrombin. The transition state of cleavage for PAR4 is substantially higher than PAR1 as a reflection of the lack of an allosteric effect induced by occupancy at exosite I for PAR4.

What is the biological significance of these different kinetic and thermodynamic pathways that PAR1 and PAR4 use to interact with thrombin? During platelet activation, PAR1 and thrombin are present at near stoichiometric amounts, since only 600–1800 PAR1 receptors ($\approx$1 nM) are expressed on the surface of each platelet [32,33]. Therefore, the PAR1 receptor with its high-affinity Hir [30] is optimally constructed to grab and hold low concentrations of thrombin [34] using its fast association rate and efficient active site-locking mechanism [11]. Once the exodomain is cut, thrombin can remain associated with PAR1 through the Hir–exosite I interaction [11], leaving its active site free to potentially interact with a nearby PAR4 [29]. The anionic motif of PAR4 may interact with the positively charged groups at or near exosite I of thrombin [5] to increase affinity either in the presence or absence of PAR1. Because PAR4 does not use a Hir-docking mechanism, its P_4-P_1 sequence may bind unencumbered to the active site of thrombin still tethered to the cleaved PAR1 receptor. This macromolecular process may be enhanced by dimerization of PAR1 and PAR4 as is suggested by the co-factoring that occurs between PAR3 and PAR4 on murine platelets [20].

We thank Odessa Yabut and Christopher Singh for their assistance in plasmid construction and Lidija Covic for helpful discussions. This work was supported in part by a Fellow Scholar Award from the American Society of Hematology (S. L. J.) and by National Institutes of Health grant no. R01HL57905 (A. K.).

REFERENCES

1 Covic, L., Gresser, A. L. and Kuliopulos, A. (2000) Biphasic kinetics of activation and signaling for PAR1 and PAR4 thrombin receptors in platelets. Biochemistry **39**, 5458–5467
2 Shapiro, M. J., Weiss, E. J., Faruqi, T. R. and Coughlin, S. R. (2000) Protease-activated receptors 1 and 4 are shut off with distinct kinetics after activation by thrombin. J. Biol. Chem. **275**, 25216–25221
3 Mathews, I. I., Padmanabhan, K. P., Ganesh, V., Tulinsky, A., Ishii, M., Chen, J., Turck, C. E., Coughlin, S. R. and Fenton, J. W. (1994) Crystallographic structures of thrombin complexes with thrombin receptor peptides: existence of expected and novel binding modes. Biochemistry **33**, 3266–3279
4 Hall, S. W., Nagashima, M., Zhao, L., Morser, J. and Leung, L. L. K. (1999) Thrombin interacts with thrombomodulin, protein C, and thrombin-activatable fibrinolysis via specific and distinct domains. J. Biol. Chem. **274**, 25510–25516
5 Ayala, Y. M., Cantwell, A. M., Rose, T., Bush, L. A., Arosio, D. and DiCera, E. (2001) Molecular mapping of thrombin-receptor interactions. Proteins **45**, 107–116
6 Dharmawardana, K. R., Olson, S. T. and Bock, P. E. (1999) Role of regulatory exosite I in binding of thrombin to human factor V, factor Va, factor Va subunits, and activation fragments. J. Biol. Chem. **274**, 18635–18643
7 Hall, S. W., Gibbs, C. S. and Leung, L. L. K. (2001) Identification of critical residues on thrombin mediating its interaction with fibrin. Thromb. Haemost. **86**, 1466–1474
8 Boskovic, D. S. and Krishnaswamy, S. (2000) Exosite binding tethers the macromolecular substrate to the prothrombinase complex and directs cleavage at two spatially distinct sites. J. Biol. Chem. **275**, 38561–38570
9 Baugh, R. J., Dickinson, C. D., Ruf, W. and Krishnaswamy, S. (2000) Exosite interactions determine the affinity of factor X for the extrinsic Xase complex. J. Biol. Chem. **275**, 28826–28833
10 Liu, L. W., Vu, T., Esmon, C. T. and Coughlin, S. R. (1991) The region of the thrombin receptor resembling hirudin binds to thrombin and alters enzyme specificity. J. Biol. Chem. **266**, 16977–16980
11 Jacques, S. L., LeMasurier, M., Sheridan, P. J., Seeley, S. K. and Kuliopulos, A. (2000) Substrate-assisted catalysis of the PAR1 thrombin receptor: enhancement of macromolecular association and cleavage. J. Biol. Chem. **275**, 40671–40678
12 Xu, W.-F., Andersen, H., Whitmore, T. E., Presnell, S. R., Yee, D. P., Ching, A., Gilbert, T., Davie, E. W. and Foster, D. C. (1998) Cloning and characterization of human protease-activated receptor 4. Proc. Natl. Acad. Sci. U.S.A. **95**, 6642–6646
13 Kahn, M. L., Zheng, Y.-W., Huang, W., Bigornia, V., Zheng, D., Moff, S., Farese, R. V., Tam, C. and Coughlin, S. R. (1998) A dual thrombin receptor system for platelet activation. Nature (London) **394**, 690–694
14 Covic, L., Gresser, A. L., Talavera, J., Swift, S. and Kuliopulos, A. (2002) Activation and inhibition of G protein-coupled receptors by cell-penetrating membrane-tethered peptides. Proc. Natl. Acad. Sci. U.S.A. **99**, 643–648
15 Kuliopulos, A., Covic, L., Seeley, S. K., Sheridan, P. J., Helin, J. and Costello, C. E. (1999) Plasmin desensitization of the PAR1 thrombin receptor: kinetics, sites of truncation, and implications for thrombolytic therapy. Biochemistry **38**, 4572–4585
16 Kuliopulos, A., Talalay, P. and Mildvan, A. S. (1990) Combined effects of two mutations of catalytic residues on the ketosteroid isomerase reaction. Biochemistry **29**, 10271–10280
17 Cleland, W. W. (1990) Steady state kinetics. In The Enzymes, vol. 19 (Boyer, P.D., ed.), pp. 99–158, Academic Press, New York
18 Hopfner, K.-P. and DiCera, E. (1992) Energetics of thrombin-fibrinogen interactions. Biochemistry **31**, 11567–11571
19 Ishii, K., Gerszten, R., Zheng, Y. W., Welsh, J. B., Turck, C. W. and Coughlin, S. R. (1995) Determinants of thrombin receptor cleavage. J. Biol. Chem. **270**, 16435–16440
20 Nakanishi-Matsui, M., Zheng, Y.-W., Sulciner, D. J., Weiss, E. J., Ludeman, M. J. and Coughlin, S. R. (2000) PAR3 is a cofactor for PAR4 activation by thrombin. Nature (London) **404**, 609–613
21 Lottenberg, R., Hall, J. A., Blinder, M., Binder, E. P. and Jackson, C. M. (1983) The action of thrombin on peptide p-nitroanilide substrates. Substrate selectivity and examination of hydrolysis under different reaction conditions. Biochim. Biophys. Acta **742**, 539–557
22 Harris, J. L., Backes, B. J., Leonetti, F., Mahrus, S., Ellman, J. A. and Craik, C. S. (2000) Rapid and general profiling of protease specificity by using combinatorial fluorogenic substrate libraries. Proc. Natl. Acad. Sci. U.S.A. **97**, 7754–7759
23 Backes, B. J., Harris, J. L., Leonetti, F., Craik, C. S. and Ellman, J. A. (2000) Synthesis of positional-scanning libraries of fluorogenic peptide substrates to define the extended substrate specificity of plasmin and thrombin. Nat. Biotechnol. **18**, 187–193
24 Cleary, D. B., Trumbo, T. A. and Maurer, M. C. (2002) Protease-activated receptor 4-like peptides bind to thrombin through an optimized interaction with the enzyme active site surface. Arch. Biochem. Biophys. **403**, 179–188
25 Duffy, E. J., Angliker, H., LeBonniec, B. F. and Stone, S. R. (1997) Allosteric modulation of the activity of thrombin. Biochem. J. **321**, 361–365
26 Shi, F., Hogg, P. J., Winzor, D. J. and Jackson, C. M. (1998) Evidence for multiple enzyme site involvement in the modulation of thrombin activity by products of prothrombin proteolysis. Biophys. Chem. **75**, 187–199
27 Hogg, P. J. and Jackson, C. M. (1990) Formation of a ternary complex between thrombin, fibrin monomer, and heparin influences the action of thrombin on its substrates. J. Biol. Chem. **265**, 248–255
28 Rydel, T. J., Ravichandran, K. G., Tulinski, A., Bode, W., Huber, R., Roitsch, C. and Fenton, II, J. W. (1990) The structure of a complex of recombinant hirudin and human α-thrombin. Science **249**, 277–280
29 Seeley, S., Covic, L., Jacques, S. L., Sudmeier, J., Baleja, J. D. and Kuliopulos, A. (2003) Structural basis for thrombin activation of a protease-activated receptor: inhibition of intramolecular liganding. Chem. Biol. **10**, in the press
30 Vu, T.-K. H., Wheaton, V. I., Hung, D. T., Charo, I. and Coughlin, S. R. (1991) Domains specifying thrombin-receptor interaction. Nature (London) **353**, 674–677
31 Vindigni, A., Dang, Q. D. and DiCera, E. (1997) Site-specific dissection of substrate recognition by thrombin. Nat. Biotechnol. **15**, 891–895
32 Brass, L. F., Vassallo, R. R., Belmonte, I., Ahoja, M., Cichowski, K. and Hine, J. A. (1992) Structure and function of the human platelet thrombin receptor. J. Biol. Chem. **267**, 13795–13798
33 Ahn, H.-S., Foster, C., Boykow, G., Arik, L., Smith-Torhan, A., Hesk, D. and Chatterjee, M. (1997) Binding of a thrombin receptor tethered ligand analogue to human platelet thrombin receptor. Mol. Pharmacol. **51**, 350–356
34 Rand, M. D., Lock, J. B., Veer, C. V., Gaffney, D. P. and Mann, K. G. (1996) Blood clotting in minimally altered whole blood. Blood **88**, 3432–3445
35 Fersht, A. (1985) in Enzyme Structure and Mechanism, pp. 311–346, W. H. Freeman and Company, New York

Received 26 June 2003/9 September 2003; accepted 18 September 2003
Published as BJ Immediate Publication 18 September 2003, DOI 10.1042/BJ20030954

© 2003 Biochemical Society